Radiological Physics and Technology
https://doi.org/10.1007/s12194-018-0486-x

Potentials of radiomics for cancer diagnosis and treatment in comparison with computer-aided diagnosis

Hidetaka Arimura[1] · Mazen Soufi[2] · Kenta Ninomiya[4] · Hidemi Kamezawa[3] · Masahiro Yamada[4]

Received: 1 October 2018 / Revised: 14 October 2018 / Accepted: 17 October 2018

Abstract
Computer-aided diagnosis (CAD) is a field that is essentially based on pattern recognition that improves the accuracy of a diagnosis made by a physician who takes into account the computer's "opinion" derived from the quantitative analysis of radiological images. Radiomics is a field based on data science that massively and comprehensively analyzes a large number of medical images to extract a large number of phenotypic features reflecting disease traits, and explores the associations between the features and patients' prognoses for precision medicine. According to the definitions for both, you may think that radiomics is not a paraphrase of CAD, but you may also think that these definitions are "image manipulation". However, there are common and different features between the two fields. This review paper elaborates on these common and different features and introduces the potential of radiomics for cancer diagnosis and treatment by comparing it with CAD.

Keywords Radiomics · Computer-aided diagnosis · Cancer diagnosis and treatment · Precision medicine

1 Introduction

Is "radiomics" just a paraphrase of "computer-aided diagnosis (CAD)"? The authors claim that there are common and different features between "current" radiomics and "conventional" CAD. Table 1 shows the comparisons of current radiomics with conventional CAD, which will gradually be changing.

CAD has dealt with issues of radiological diagnosis such as missed or misunderstood lesions in terms of detection and differentiation [1–3]. On the other hand, radiomics addresses the issues of precision medicine [4, 5], which is a treatment strategy for making decisions about molecularly targeted agents based on genetic mutations rather than affected organs. However, there have been several issues with regard to precision medicine, e.g., the necessity for invasive biopsy, additional cost, and slow throughput procedures [6]. In addition, the information obtained from small pieces of heterogeneous tumor tissues extracted from a single biopsy specimen or from a blood sample could be inaccurate, because gene-expression signatures associated with good and poor prognoses may be detected in different regions of the same tumor [7]. The gene-expression signature is a set or combined set of genes in a cell with a unique pattern of gene expression [8] and is considered prognostic biomarker. In contrast, medical images and their corresponding image features have great potential to capture possibly "entire" and prognostic information on intratumoral heterogeneity in non-invasive, low-cost, and rapid ways.

The purpose of CAD is to detect and/or differentiate among diseases, e.g., detection of lung cancer and differentiation of Alzheimer's disease. CAD has generally been defined as a diagnosis made by a physician, who takes into account computer outputs based on quantitative analyses (e.g., detecting or/and diagnosing lesions) of radiological images [1–3].

Radiomics aims to discover prognostic signatures extracted from multimodality images for decision making

✉ Hidetaka Arimura
arimurah@med.kyushu-u.ac.jp

1 Division of Medical Quantum Science, Department of Health Sciences, Faculty of Medical Sciences, Kyushu University, 3-1-1, Maidashi, Higashi-ku, Fukuoka 812-8582, Japan

2 Division of Information Science, Nara Institute of Science and Technology, Ikoma, Japan

3 Department of Radiological Technology, Faculty of Fukuoka Medical Technology, Teikyo University, Omuta, Japan

4 Division of Medical Quantum Science, Department of Health Sciences, Graduate School of Medical Sciences, Kyushu University, Fukuoka, Japan

Published online: 29 October 2018

Table 1 A comparison between current radiomics and conventional CAD

Item	Radiomics	CAD
Addressed issues	Issues in precision medicine	Issues in radiological diagnosis
Major purpose	Discovery of signatures (imaging biomarkers) for prognostic prediction or subtype classification	Development of methods for detection or differentiation of diseases
Fundamental approach	Data science including pattern recognition and image processing	Pattern recognition with image processing
Related field	Biology (omics), radiology, radiotherapy, pathology	Radiology and pathology
Logical reasoning	Inductive (data driven)	Deductive (algorithm driven)
Types of data	General medical images with histological images and omics data	General medical images with histological images

of treatment-related actions such as treatment policies (e.g., surgery, radiotherapy, chemotherapy, and immune therapy) [4, 5]. The prognostic signatures could extensively characterize cancer traits from the standpoint of medical imaging and predict patients' prognoses. Therefore, the prognostic signatures are considered "surrogate imaging biomarkers". The signatures are represented mathematically as vectors consisting of significant image features associated with patients' prognoses. A number of imaging biomarkers based on radiomics in radiation therapy have been explored by assessment of several end points that indicate the feasibility of radiomics such as overall survival and disease-free survival of patients [9].

In my opinion, the fundamental approach of conventional CAD is algorithmically based on pattern recognition for developing diagnostic systems deductively [10]. Pattern recognition is the act of extracting features from objects (e.g., lesions) in the form of raw data and making a decision based on a classifier output, e.g., classifying each object into one of the possible categories of various patterns [11]. Many types of CAD systems or basic methodologies, including CADe (detection) of lung cancer, breast cancer microcalcifications, intracranial aneurysms [1], CADx (diagnosis or differentiation) of breast cancer and Alzheimer's disease [10, 12], temporal subtraction techniques [13], similar image techniques [14], and CADx for pathological images [15], have been developed in the radiological and pathological fields. Computer-assisted radiotherapy (CART) is a field similar to CAD that is based on pattern recognition and image processing for research on approaches for assisting radiation oncology staffs by providing useful information on diagnosis, treatment planning, treatment execution, and follow-up [16].

On the other hand, the fundamental approach of radiomics is based on data science that inductively and comprehensively analyzes a large number of medical images by extracting a large number of phenotypic features reflecting disease traits, and exploring the associations between imaging signatures and patients' prognoses [17]. The purpose of data science is to understand "what the data say", i.e., the underlying theory or mechanism, by extracting important patterns and trends from comprehensive analyses of big data [18]. Figure 1 depicts the data science life cycle, which is utilized for radiomics. First, the data are comprehensively collected and processed. Second, the data are analyzed using statistical techniques and/or machine learning. Third, the underlying theory in the data is discovered by visualizing the data. Finally, a validation test is performed for a dataset different from a training dataset. If the results do not satisfy a certain criteria, the cycle will be repeated.

In a definition of the authors, data science is an interdisciplinary field that includes mathematics, computer science, and domain knowledge such as medical physics and radiological sciences, to discover inductively features or hidden meaningful patterns of natural, human, and social phenomena by analyzing a vast amount of multidimensional data (big data). Similarly, the goal of radiomics is to discover prognostic signatures, which have strong associations with patients' prognoses, as meaningful patterns, i.e., imaging biomarkers.

The radiomics is a compound word of 'radio', which refers to radiological images (medical images in a broad sense), and 'omics' [6, 17]. The omics includes several study fields (genomics, transcriptomics, proteomics, and metabolomics) for understanding the biology and clinical management of a disease (e.g., cancer) by inductively and comprehensively analyzing the huge quantity of omics data [19]. The image features in radiomics are dealt with

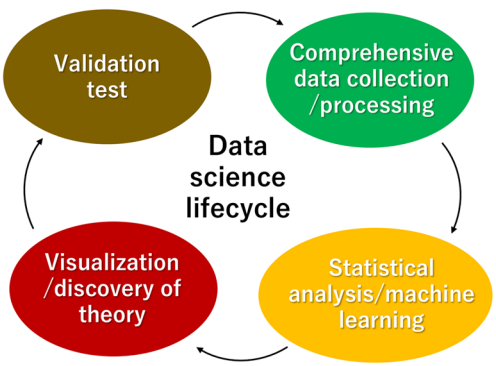

Fig. 1 Data science life cycle, which is utilized for radiomics

as omics-wise information like gene or protein. To provide insight into radiomics, the rest of this review paper consists of: 2. Fundamental approaches of radiomics, 3. Procedure of radiomic analysis, 4. Prediction of prognosis prior to treatment using radiomics, and 5. Future of radiomics and CAD.

2 Fundamental approaches of radiomics

Figure 2 is a flowchart of general CAD approaches, which consist of extraction and selection of image features within a lesion using image processing [20], statistical learning [18], and detection and/or differentiation of a lesion using classifiers (or machine learning) [20]. Figure 3 depicts flowcharts of discovery and test steps for general radiomics. In the discovery step, the extraction and selection of image features are the steps in common between CAD and radiomics. In radiomics, a huge number of image features including shape, histogram, and texture features (e.g., more than 400) are extracted from medical images for stratification of the patients. Significant features are chosen by means of repeatability and reproducibility tests [21–23] and further filtered through feature selection methods [18]. The patients are stratified into several subtypes by using a clustering method (e.g., simple thresholding with medians of image features) [6, 18]. The prognostic powers of the features were investigated specifically using a Kaplan–Meier survival analysis [24] or a Cox's proportional hazards model [25], in which significant features reflecting the prognoses should be chosen as a subset of significant features (a signature). The test step, therefore, indicates that patients' prognoses could be predicted by use of simply signatures or generally machine learning, and physicians would make decisions on treatment policies for patients.

3 Procedure of radiomic analysis

3.1 Extraction of image features

Three major types of mathematical feature models, i.e., shape, histogram, and texture features, have been utilized in the radiomics field [17].

Shape features include diameter, surface area, surface-area-to-volume ratio, sphericity, spherical disproportion, compactness, and others [26]. Histogram-based statistical features represent the overall heterogeneity using a graylevel histogram within the tumor without spatial information. Texture features are calculated from a graylevel co-occurrence matrix (GLCM) [27], graylevel run-length matrix (GLRLM) [28], neighborhood gray-tone difference matrix (NGTDM) [29], and graylevel size zone matrix (GLSZM) [30], which represent various types of local spatial inhomogeneities in terms of graylevels within a tumor. The GLSZM features were initially used for portraying the inhomogeneity of cell nuclei [30]. Since the image features depend on the quantization levels of medical images, optimal quantization levels should be investigated for the purpose and image type using reliability indices such as an intraclass correlation coefficient (ICC) [22, 23], which could reflect both the degrees of correlation and the agreement between measurements. According to our research [31], based on the ICC of the radiomic features, the optimal number of quantization levels for deriving radiomic features of lung cancer in two-dimensional (2D) dynamic electronic portal imaging device (EPID) images was 64 levels [31], whereas in 3D static computed tomography (CT) images, Shafiq-Ul-Hassan et al. [32] recommended the normalization of the texture features based on the number of quantization levels to improve their stability. In a different study, we found that the optimal number of quantization levels for computation

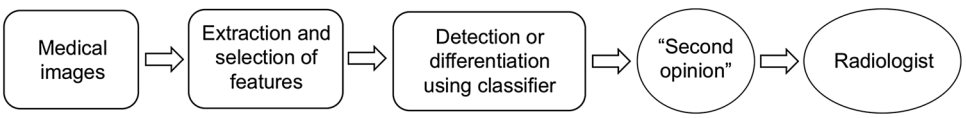

Fig. 2 A flowchart for conventional computer-aided diagnosis (CAD) systems

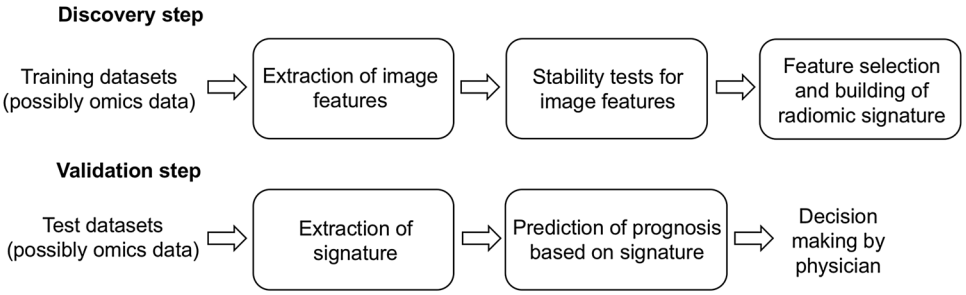

Fig. 3 Flowcharts of discovery and validation steps for general radiomics

of wavelet decomposition-based features in CT images of lung cancer was 128 levels [33].

Shafiq-Ul-Hassan et al. [32] found that some of the radiomic features depended on the voxel size and the number of quantization levels. These dependencies can be reduced or removed by introducing normalizing factors in their definitions [32].

One of the powerful mathematical tools in radiomics is the 2D or 3D fast discrete wavelet transformation (fDWT) [34], which can decompose multiscale local intensity variations (intratumoral heterogeneity) in an image into several low- and high-frequency components [35]. The decompositions at different scales are performed by convolving the images with mother wavelets (basis functions) in a single down-sampling step at each direction of x, y, and z axes, which has been known as the 'wavelet analysis filter bank' approach [34, 35]. The mother wavelets have multiple characteristics that have impacts on the computation of radiomic features, particularly the texture features on wavelet-transformed images [36]. Therefore, we attempted to identify the optimal mother wavelets among 31 mother wavelets (5 Daubechies, 3 Coiflet, 7 Biorthogonal, 8 Reverse Biorthogonal, 4 Symlet, 4 Fejer-Korovkin) in the survival prediction of lung cancer patients with use of wavelet-decomposition-based (WDB) radiomic features in CT images [33]. Symlet and Biorthogonal mother wavelets could have the potential to predict the survival of lung cancer patients by using WDB radiomic features in CT images [33].

Oakden-Rayner et al. [37] compared two approaches for the prediction of 5-year mortality with deep learning as well as three types of machine learning classifiers (random forests, support vector machines and boosted tree algorithms) trained on the human-defined image features. They believe that deep learning can automatically create optimal low- and high-level features as mentioned by the Hinton's review paper [38]. The areas under the curve (AUC) for predicting 5-year mortality were 0.677 ± 0.214 with deep learning and 0.646 ± 0.255 with human-defined features [37], where p values were not shown. The results showed still low AUC, so that it cannot be concluded that deep learning can produce image features superior to conventional features. Ning et al. [39] proposed a hybrid system that includes different features selected with the radiomics model and convolutional neural networks (CNNs) and that integrates both features to deal with the classification of gastrointestinal stromal tumors (GISTs). The radiomics model and CNNs were constructed for producing global radiomics and local convolutional features, respectively. The classification performance of the combined features was an AUC of 0.882, which outperformed those of radiomics (AUC: 0.807) and CNNs (AUC: 0.826) approaches.

Shen et al. [40] compared the prognostic performance between 2D and 3D radiomics features in CT images of non-small cell lung cancer (NSCLC). They concluded that both 2D and 3D CT radiomics features had a certain prognostic ability in NSCLC, but 2D features indicated a better performance. 2D features may be preferable from the point of view of the calculation cost.

3.2 Stability tests for image features

Stable radiomic features should be selected based on repeatability and reproducibility tests.

Repeatability or test–retest reliability is the closeness of the agreement between the results of successive measurements of the same measurand carried out under the same conditions of measurement (same measurement procedure, same observer, same measuring instrument, used under the same conditions, in the same location, with repetition over a short period of time) [41]. The reproducibility refers to the closeness of the agreement between the results of measurements of the same measurand carried out under changed conditions of measurement (principle of measurement, method of measurement, observer, measuring instrument, reference standard, location, conditions of use, time) [41].

Repeatable and reproducible features are chosen by using evaluation indices such as ICC [22, 23] or the concordance correlation coefficient (CCC) [23] computed on a test–retest and multiple segmentation datasets, respectively [33]. The publicly available online Reference Image Database to Evaluate Response (RIDER) non-small cell lung cancer (NSCLC) dataset on The Cancer Imaging Archive (TCIA) [42, 43] can be employed as the test–retest dataset for the repeatability test [5, 21, 31, 33]. In the RIDER database, patients were scanned twice (test–retest setting) with an interval of 15 min. A multiple-segmentation dataset in TCIA, including images obtained from several institutions, is available for testing the reproducibility [44, 45]. Each CT image includes several contours on each lung tumor region that was delineated by using different initial conditions of an algorithm at several institutions [33].

Berenguer et al. reported that the majority (94%) of the evaluated radiomics features for CT images were not reproducible and were redundant [46]. If all of the CT imaging parameters were held constant, a smaller percentage (6%) of the radiomics features were reproducible and contained independent information.

Bologna et al. [47] developed a way to assess the stability and discrimination capacity of radiomic features on apparent diffusion coefficient (ADC) maps without the need of test–retest or multiple delineations. Geometrical transformations (translations) of increasing entity were applied to the regions of interest (ROIs). The ICC was used to compare the features computed on the original and modified ROIs. The results suggested that the observed radiomic features are

mainly stable and discriminative, but the stability depends on the region of the body under observation.

Soufi et al. [31] explored the temporal stability of radiomic features in the presence of tumor motion in EPID images and the prognostic powers of temporally stable features. Fifteen radiomic features were found to be temporally stable at various quantization levels. Among these features, seven features have shown potentials for prognostic prediction in lung cancer patients.

3.3 Building of radiomic signatures

The major purposes of radiomics are the discovery of signatures (imaging biomarkers) for prognostic prediction or subtype classification by measuring a large number of image features on a massive number of medical images as shown in Table 1. Even though unstable features are excluded by using the repeatability and reproducibility tests, the number of image features n could be larger than the number of observations N (e.g., number of patients), and some features may be redundant. Consequently, you may have an overfitting problem in prediction models with training data, which may produce large prediction errors in test data [18]. Therefore, to increase the prediction accuracy and model interpretation [18], the number of features n should be reduced to a relatively smaller number compared with N, possibly $n < N/10$ [48, 49]. In other words, significant and independent features should be selected subject to small prediction errors and $n < N/10$. Besides, Chow et al. suggested a formula of a sample size estimation for Cox's proportional hazards regression model [50].

A simple feature selection method for discovery of the radiomic signatures is to evaluate the p values of statistically significant differences between the survival curves of two patient subgroups with either better or worse prognoses. The patients were stratified by thresholding a specific radiomic feature and could have different responses to the same treatment approach. Figure 4 shows the survival curves for high- and low-risk patients, which were determined based on a median of a radiomic feature (coarseness derived from NGTDM). Figure 5 shows the image features with prognostic power based on p values. The image features showing p values smaller than 0.05 ($-\log_{10}(p \text{ value})$ larger than 1.3) could be considered significant features of radiomic signatures.

In addition, the image features can be chosen based on the association with patients' prognoses. The signature is defined as a feature subset including significant features (like gene expression in the omics field). Many feature selection methods, e.g., Wilcoxon test-based feature selection method [51], Coxnet, elastic net [52], least absolute shrinkage and selection operator (LASSO) [53], feature selection method of joint mutual information [54], or logistic regression [55], have been

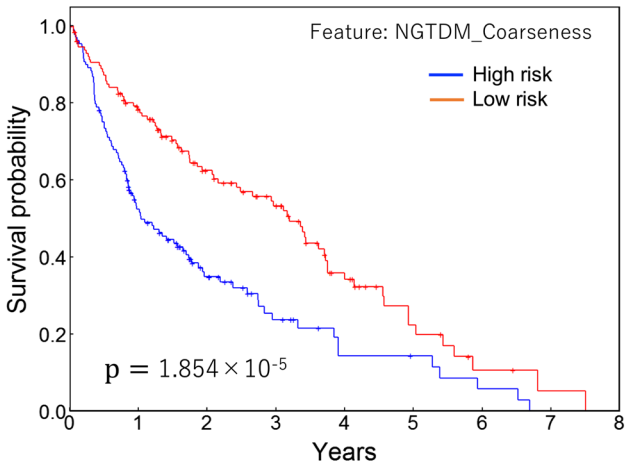

Fig. 4 Survival curves for high- and low-risk patients, which were determined based on a median of a radiomic feature (coarseness from NGTDM)

employed with machine learning techniques. Several combinations of feature selection methods with machine learning techniques were comprehensively compared with each other, because the most appropriate combinations for discovering signatures with prognostic powers depend on objectives and imaging modalities.

The feasibilities of shrinkage methods including LASSO, elastic net, and Coxnet have been proved in several studies [52, 53, 55]. In particular, Coxnet is a powerful algorithm based on Cox's proportional hazards model [25] for finding the significant feature subsets (predictors) that have an impact on survival times. In Coxnet algorithm, Cox's proportional hazards model with the radiomic signature (feature vector with a length of n) $\boldsymbol{x_i} \in R^n$, where n is the number of image features and i is the patient number, is optimized by maximizing a partial likelihood. Cox's proportional hazards model $h_i(t)$ for a patient i at a time t can be expressed as:

$$h_i(t) = h_o(t)e^{\boldsymbol{x_i}^T\boldsymbol{\beta}}, \tag{1}$$

where $h_o(t)$ is the baseline hazard function, and $\boldsymbol{\beta}$ is the coefficient's vector with a length of n. To maximize the partial likelihood subject to a convex combination of L1 and L2 norm penalties (elastic net penalty), the Lagrangian formulation is constructed as follows [56]:

$$\hat{\boldsymbol{\beta}} = \arg\max_{\boldsymbol{\beta}} \left[k(\log \text{ (partial likelihood)}) - \lambda P_\alpha(\boldsymbol{\beta})\right], \tag{2}$$

where

$$P_\alpha(\boldsymbol{\beta}) = \alpha\|\boldsymbol{\beta}\|_1 + \frac{1-\alpha}{2}\|\boldsymbol{\beta}\|_2^2, \tag{3}$$

k is the scaling factor, $\|\cdot\|_1$ indicates the L_1 norm (LASSO penalty term), $\|\cdot\|_2$ indicates the L_2 norm (ridge regression penalty term), λ is the Lagrange multiplier, and $\alpha \in [0, 1]$

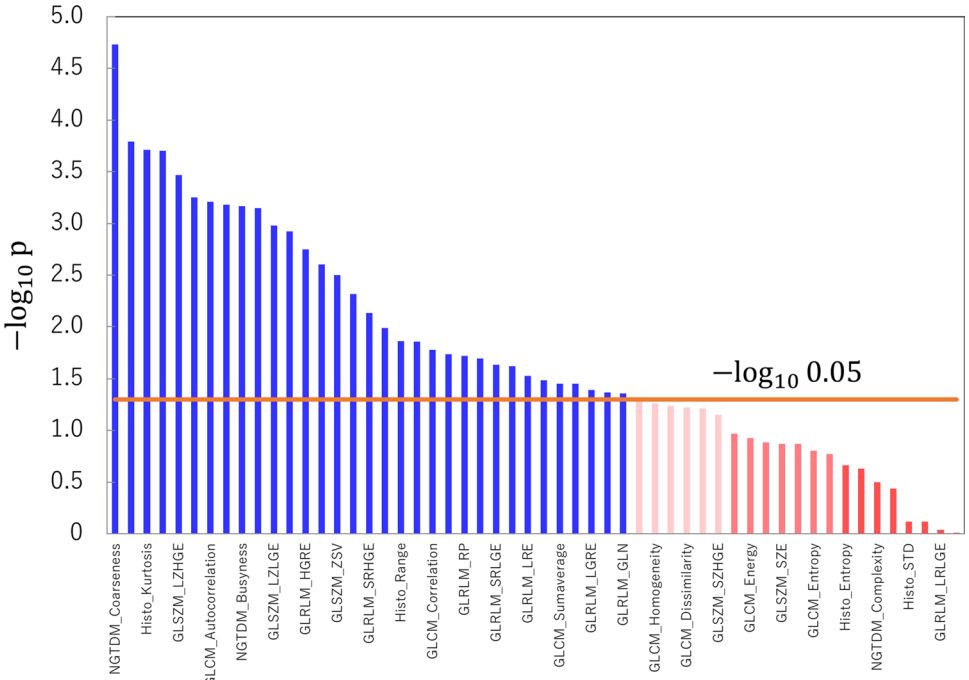

Fig. 5 Image features with prognostic powers based on p values. The lower p values (stronger prognostic power) indicate a larger $-\log_{10}p$ value

is the blending parameter for adjusting the impacts of the LASSO and ridge regression penalties on the overall regularization. A value $\alpha = 0$ reduces the penalization into a ridge regression, and thus all of the radiomic features are included in the model. A value of $\alpha = 1$ reduces the penalization to the LASSO term, thereby reducing the number of the features by 'shrinking' the coefficients of highly correlated features to zero.

Soufi et al. [33] identified the optimal mother wavelets based on maximization of a ranking index (RI) incorporating Coxnet prediction error and the summation of the p values of the radiomic features in Cox's proportional hazards model on training datasets. The prognostic performance of the optimal mother wavelets was validated based on the concordance index (CI) of the Cox's proportional hazards models. They revealed the potential of Symlet and Biorthogonal mother wavelets in the survival prediction for lung cancer patients.

Recently, deep learning algorithms have been widely used as one of the more useful tools for segmentation, extraction, and selection of image features, and for prediction of prognosis in the medical imaging field including CAD, radiomics, medical image analysis [57–59], and CART [60]. Deep learning is a type of mapping function $\boldsymbol{f}(\cdot)$ from input image vectors $\{\boldsymbol{x}_j\}$ (j: input vector number) to output vectors $\boldsymbol{y} = \boldsymbol{f}(\boldsymbol{x}_j, \boldsymbol{w})$ ($\boldsymbol{w}$: weight vector) [61]. Therefore, you may think that most of the approaches except the production of input images can be replaced by deep learning. However, the authors believe that the entire discovery step should not be replaced, because the deep learning thus far cannot inherently distinguish "causation" from "correlation" [62] in the mapping functions. According to the results of deep learning, you may mistakenly consider "correlation" as "causation", which are quite different from each other. If the purpose of your research is to find the "reason" or "cause" of the phenomena, deep learning might be inappropriate.

4 Prediction of prognosis prior to treatment using radiomics

Patients' prognoses such as therapy responses can be predicted prior to treatment by imaging biomarkers derived from radiomics schemes. Qin et al. [63] investigated the utility of image features of the GLCM based on intravoxel incoherent motion diffusion-weighted imaging (IVIM-DWI) (81 patients) for predicting the early response to chemoradiotherapy for nasopharyngeal carcinoma (NPC). GLCM features based on IVIM-DWI, especially on a diffusion-related map, may be a potential tool for predicting the early response of NPC before starting chemoradiotherapy.

Wang et al. [64] evaluated the ability of MR imaging radiomics for pretreatment prediction of the response to induction chemotherapy (IC) in 120 patients with NPC. The association between the early response and the radiomics signatures obtained from the LASSO logistic regression model to the IC was explored. For stratification of the patients into responders and non-responders, the radiomic score of each patient was calculated by use of linear combinations of radiomic features weighted by coefficients from LASSO. As imaging biomarkers, the radiomics signatures

may provide valuable and practical approaches to the characterization of individual patients to guide each treatment.

Cui et al. [65] developed and validated a radiomics nomogram incorporating multiparametric MRI-based radiomics signature and clinical factors for the preoperative prediction of pathological complete responses of 186 patients with locally advanced rectal cancer (LARC). They also derived the radiomic signature from LASSO and calculated the radiomics scores to be used for the nomogram. This study suggested that the pretreatment radiomics nomogram could predict the complete responses in patients with LARC and potentially guide treatments to select patients for a "wait-and-see" policy.

Crispin-Ortuzar et al. [66] proposed a method for predicting the hypoxia status by use of a combination of contrast-enhanced computed tomography and [^{18}F]-fluorodeoxyglucose positron emission tomography (^{18}F-FDG PET) radiomic features in 121 lesions from 75 head and neck cancer patients. Seventy-nine lesions were used for training a cross-validated LASSO regression model based on radiomics features, whereas the remaining 42 lesions were held out as an internal test subset. A radiomics signature built from hypoxia imaging ^{18}F-FDG PET and contrast-enhanced CT features correlated with the maximum tumor-to-blood uptake ratio of ^{18}F-fluoromisonidazole (FMISO) PET in head and neck cancer patients. The ^{18}F-FDG-PET imaging biomarker could be useful for personalization of head and neck cancer treatment at centers without the use of ^{18}F-FMISO PET.

Larue et al. [67] explored the prognostic value of radiomics in CT images of esophageal cancer patients. They hypothesized that radiomics features could contain prognostic information in addition to the conventional baseline clinical variables: gender, age, histology, and cTNM-stage, as well as the tumor regression grade (TRG) after neoadjuvant treatment. To verify the hypothesis, they trained and externally validated two random forest (RF) models (radiomics-based and clinical-data-based models) to predict 3-year overall survival after the treatment of 'Dutch Chemo-Radiotherapy for Oesophageal cancer followed by Surgery Study' based on either radiomics or clinical variables. In the validation dataset, the radiomic RF model yielded an AUC of 0.61 (95% CI 0.47–0.75), whereas the clinical RF model resulted in an AUC of 0.62 (95% CI 0.49–0.76).

Hou et al. [68] reported on a radiomics method for predicting the treatment response to chemoradiotherapy (responders: patients with complete response and partial response; non-responders: patients with stable disease) in esophageal squamous cell carcinoma by use of T2-weighted and spectral attenuated inversion-recovery (SPAIR) T2-weighted MR images. The artificial neural network (ANN) and support vector machine (SVM) based on image features extracted from the SPAIR T2-weighted sequence (SVM: 0.929, ANN: 0.883) showed a higher accuracy than those based on the T2-weighted sequence (SVM: 0.893, ANN: 0.861).

Shiradkar et al. [54] identified a signature derived from pretreatment bi-parametric MR images (T2-weighted images and ADC maps of 120 patients) that may be predictive of prostate cancer biochemical recurrence (BCR). The BCR is the rise in the blood level of prostate-specific antigen in prostate cancer patients after treatment with surgery or radiation therapy. They employed three classifiers and three feature selection methods and found that SVM with joint mutual information produced the highest AUC of 0.73 for a validation dataset in the classification of BCR+ and BCR−.

5 Future of radiomics and CAD

As shown in Table 1, there are some differences between "conventional" CAD and "current" radiomics such as background and purpose, but both share common parts of image processing, feature extraction, feature selection, and classifiers. CAD has a history of more than 30 years, and its research field has accumulated abundant knowledge about it. Therefore, radiomics could accelerate precision medicine by standing on the shoulders of the giant of CAD.

The authors found several studies indicating some synergistic effects between CAD and radiomics. Gangeh et al. [69] developed a computer-aided prognosis method for cell death categorization and prediction in vivo by using quantitative ultrasound images and machine learning techniques. Giannini et al. [70] assessed whether a proposed CAD system can predict a pathological complete response to neoadjuvant chemotherapy prior to treatment by using texture features. Kai et al. [71] developed a radiogenomic CAD scheme to support personalized medicine by using a classifier to learn changes in image features of a lesion related to the difference between genotypes.

Radiogenomics [5] is a promising field to develop imaging biomarkers incorporating both phenotypic and genotypic metrics that can predict patient outcomes, and thus can better stratify patients for more precise therapeutic care in precision medicine than the radiomics [72]. The phenotypic features correlating with genotypes can be utilized as surrogate markers of the genotypes. Furthermore, a more advanced concept of panomics [73, 74] rather than radiomics has been suggested as a new omics field to discover integrated data with imaging features (radiomics) and biological markers (genomics, proteomics, metabolomics) to be used for precision medicine.

Acknowledgements The researches described in this review paper were partially supported by the "Program for Supporting Educations and Researches on Mathematics and Data Science in Kyushu

University". The authors are grateful to all members of the Arimura laboratory (http://web.shs.kyushu-u.ac.jp/~arimura), whose comments made enormous contributions to the researches described in this review paper.

Compliance with ethical standards

Conflict of interest The authors declare no conflict of interest.

Human rights This article does not include studies using human subjects.

Animal rights This article does not include others studies using animal models.

References

1. Doi K. Current status and future potential of computer-aided diagnosis in medical imaging. Br J Radiol. 2005;78(1):3–19.
2. Doi K. Diagnostic imaging over the last 50 years: research and development in medical imaging science and technology. Phys Med Biol. 2006;51(13):R5–27.
3. Doi K. Computer-aided diagnosis in medical imaging: historical review, current status and future potential. Comput Med Imaging Gr. 2007;31(4–5):198–211.
4. Lambin P, Rios-Velazquez E, Leijenaar R, Carvalho S, van Stiphout RG, Granton P, Zegers CM, Gillies R, Boellard R, Dekker A, Aerts HJ. Radiomics: Extracting more information from medical images using advanced feature analysis. J Cancer. 2012;48:441–6.
5. Aerts HJ, Velazquez ER, Leijenaar RT, et al. Decoding tumour phenotype by noninvasive imaging using a quantitative radiomics approach. Nat Commun. 2014;5:4006. https://doi.org/10.1038/ncomms5006.
6. Arimura H, Soufi M. A review on radiomics for personalized medicine in cancer treatment. Med Imaging Technol. 2018;36(2):81–9.
7. Gerlinger M, Rowan AJ, Horswell S, et al. Intratumor heterogeneity and branched evolution revealed by multiregion sequencing. N Engl J Med. 2012;366:883–92.
8. Itadani H, Mizuarai S, Kotani H. Can systems biology understand pathway activation? Gene expression signatures as surrogate markers for understanding the complexity of pathway activation. Curr Genom. 2008;9(5):349–60.
9. Peeken JC, Nüsslin F, Combs SE. "Radio-oncomics": the potential of radiomics in radiation oncology. Strahlenther Onkol. 2017;193(10):767–79.
10. Arimura H, Tokunaga C, Yamashita Y, Kuwazuru K. Magnetic resonance image analysis for brain CAD systems with machine learning. In: Suzuki K, editor. Machine learning in computer-aided diagnosis: medical imaging intelligence and analysis. Hershey: IGI Global; 2012. pp. 258–96.
11. Duda RO, Hart PE, Stork DG. Pattern classification, 2nd ed. New York: Wiley-Interscience; 2000.
12. Giger ML, Chan HP, Boone J. Anniversary paper: history and status of CAD and quantitative image analysis: the role of medical physics and AAPM. Med Phys. 2008;35(12):5799–820.
13. Shiraishi J, Li Q, Appelbaum D, Doi K. Computer-aided diagnosis and artificial intelligence in clinical imaging. Semin Nucl Med. 2011;41(6):449–62.
14. Muramatsu C. Overview on subjective similarity of images for content-based medical image retrieval. Radiol Phys Technol. 2018;11(2):109–24.
15. Yamaguchi M. Computer-aided differentiation for pathology images. In: Arimura H, editor. Image-based computer-assisted radiation therapy. Singapore: Springer; 2017.
16. Arimura H. Image-based computer-assisted radiation therapy. Singapore: Springer; 2017.
17. Arimura H, Soufi M, Kamezawa H, Ninomiya K, Yamada M. Radiomics with artificial intelligence for precision medicine in radiation therapy. J Radiat Res. 2018;59:1–8 **(Epub ahead of print)**.
18. Hastie T, Tibshirani R, Friedman J. The elements of statistical learning -data mining, inference, and prediction, 2nd ed. New York: Springer; 2008.
19. Yoo BC, Kim KH, Woo SM, et al. Clinical multi-omics strategies for the effective cancer management. J Proteom. 2017;188:97–106.
20. Suzuki K. Computer-aided diagnosis: medical imaging intelligence and analysis. Hershey: IGI Global; 2012.
21. Balagurunathan Y, Kumar V, Gu Y, Kim J, Wang H, Liu Y, Goldgof DB, Hall LO, Korn R, Zhao B, Schwartz LH, Basu S, Eschrich S, Gatenby RA, Gillies RJ. Test-retest reproducibility analysis of lung CT image features. J Digit Imaging. 2014;27(6):805–23.
22. Koo TK, Li MY. A guideline of selecting and reporting intraclass correlation coefficients for reliability research. J Chiropr Med. 2016;15(2):155–63.
23. Koo TK, Li MY. Erratum to "A Guideline of Selecting and Reporting Intraclass Correlation Coefficients for Reliability Research" [J Chiropr Med. 2016;15(2):155–63]. J Chiropr Med. 2017;16(4):346.
24. Kleinbaum DG. Survival analysis: a self-learning text. New York: Springer; 1996.
25. Cox DR. Regression models and life tables (with discussion). J R Stat Soc B. 1972;34(2):187–220.
26. Bak SH, Park H, Lee HY, et al. Imaging genotyping of functional signaling pathways in lung squamous cell carcinoma using a radiomics approach. Sci Rep. 2018;8(1):3284. https://doi.org/10.1038/s41598-018-21706-1.
27. Haralick RM, Shanmugam K, Dinstein I. Textural features for image classification. IEEE Trans Syst Man Cybern. 1973;3:610–21.
28. Galloway MM. Texture analysis using gray level run lengths. Comput Gr Image Process. 1975;4:172–79.
29. Amadasun M, King R. Textural features corresponding to textural properties. IEEE Trans Syst Man Cybern. 1989;19:1264–74. https://doi.org/10.1109/21.44046.
30. Thibault G. Texture indexes and gray level size zone matrix. Application to cell nuclei classification. In: Proc. Pattern Recognition and Information Processing. Minsk, Belarus, pp. 140–145, 2009.
31. Soufi M, Arimura H, Nakamoto T, et al. Exploration of temporal stability and prognostic power of radiomic features based on electronic portal imaging device images. Phys Med Eur J Med Phys. 2018;46:32–44.
32. Shafiq-Ul-Hassan M, Zhang GG, Latifi K, Ullah G, Hunt DC, Balagurunathan Y, Abdalah MA, Schabath MB, Goldgof DG, Mackin D, Court LE, Gillies RJ, Moros EG. Intrinsic dependencies of CT radiomic features on voxel size and number of gray levels. Med Phys. 2017;44(3):1050–62.
33. Soufi M, Arimura H, Nagami N. Identification of optimal mother wavelets in survival prediction of lung cancer patients using wavelet decomposition-based radiomic features. Med Phys. 2018. https://doi.org/10.1002/mp.13202 **(Epub ahead of print)**.
34. Strang G, Nguyen T. Wavelets and filter banks. Wellesley: Wellesley-Cambridge; 1997.

35. Mallat S. A theory for multiresolution signal decomposition: the wavelet representation. IEEE Pattern Anal Mach Intell. 1989;11(7):674–93.
36. Dettori L, Semler L. A comparison of wavelet, ridgelet, and curvelet-based texture classification algorithms in computed tomography. Comp Med Biol. 2007;37(4):486–98.
37. Oakden-Rayner L, Carneiro G, Bessen T, Nascimento JC, Bradley AP, Palmer LJ. Precision radiology: predicting longevity using feature engineering and deep learning methods in a radiomics framework. Sci Rep. 2017;7(1):1648. https://doi.org/10.1038/s41598-017-01931-w.
38. LeCun Y, Bengio Y, Hinton G. Deep learning. Nature. 2015;521:436–44.
39. Ning Z, Luo J, Li Y, Han S, Feng Q, Xu Y, Chen W, Tao C, Zhang Y. Pattern classification for gastrointestinal stromal tumors by integration of radiomics and deep convolutional features. IEEE J Biomed Health Inform. 2018. https://doi.org/10.1109/JBHI.2018.2841992 **(Epub ahead of print)**.
40. Shen C, Liu Z, Guan M, Song J, Lian Y, Wang S, Tang Z, Dong D, Kong L, Wang M, Shi D, Tian J. 2D and 3D CT radiomics features prognostic performance comparison in non-small cell lung cancer. Transl Oncol. 2017;10(6):886–94.
41. JCGM 100:2008. Evaluation of measurement data—guide to the expression of uncertainty in measurement (PDF). In: Joint committee for guides in metrology; 2008.
42. Zhao B, James LP, Moskowitz CS, Guo P, Ginsberg MS, et al. Evaluating variability in tumor measurements from same-day repeat CT scans of patients with non-small cell lung cancer. Radiology. 2009;252(1):263–72.
43. Zhao B, Schwartz LH, Kris MG. Data from RIDER_Lung CT. Cancer Imaging Arch. 2015. https://doi.org/10.7937/K9/TCIA.2015.U1X8A5NR.
44. Kalpathy-Cramer J, Napel S, Goldgof D, Zhao B. Multi-site collection of lung CT data with nodule segmentations. TCIA. 2015. https://doi.org/10.7937/K9/TCIA.2015.1BUVFJR7.
45. Kalpathy-Cramer J, Mamomov A, Zhao B, Lu L, Cherezov D, et al. Radiomics of lung nodules: a multi-institutional study of robustness and agreement of quantitative imaging features. Tomography. 2016;2(4):430–7.
46. Berenguer R, Pastor-Juan MDR, Canales-Vázquez J, Castro-García M, Villas MV, Mansilla Legorburo F, Sabater S. Radiomics of CT features may be nonreproducible and redundant: influence of CT acquisition parameters. Radiology. 2018;288(2):407–15.
47. Bologna M, Corino VDA, Montin E, Messina A, Calareso G, Greco FG, Sdao S, Mainardi LT. Assessment of stability and discrimination capacity of radiomic features on apparent diffusion coefficient images. J Digit Imaging. 2018. https://doi.org/10.1007/s10278-018-0092-9 **(Epub ahead of print)**.
48. Peduzzi P, Concato J, Kemper E, Holford TR, Feinstein AR. A simulation study of the number of events per variable in logistic regression analysis. J Clin Epidemiol. 1996;49(12):1373–9.
49. Jain AK, Duin RPW, Mao J. Statistical pattern recognition [Review]. IEEE Trans Pattern Anal Mach Intell. 2000;22:4–37.
50. Chow S, Shao J, Wang H. Sample size calculations in clinical research. Chapman and Hall/CRC biostatistics series, 2nd ed. Boca Raton: CRC; 2008.
51. Parmar C, Grossmann P, Bussink J, et al. Machine learning methods for quantitative radiomic biomarkers. Sci Rep. 2015;5:13087. https://doi.org/10.1038/srep13087.
52. Leger S, Zwanenburg A, Pilz K, et al. A comparative study of machine learning methods for time-to-event survival data for radiomics risk modelling. Sci Rep. 2017;7(1):13206. https://doi.org/10.1038/s41598-017-13448-3.
53. Abdollahi H, Mostafaei S, Cheraghi S, et al. Cochlea CT radiomics predicts chemoradiotherapy induced sensorineural hearing loss in head and neck cancer patients: a machine learning and multi-variable modelling study. Phys Med Eur J Med Phys. 2018;45:192–7. https://doi.org/10.1016/j.ejmp.2017.10.008.
54. Shiradkar R, Ghose S, Jambor I, Taimen P, Ettala O, Purysko AS, Madabhushi A. Radiomic features from pretreatment biparametric MRI predict prostate cancer biochemical recurrence: preliminary findings. J Magn Reson Imaging. 2018. https://doi.org/10.1002/jmri.26178 **(Epub ahead of print)**.
55. Gabryś HS, Buettner F, Sterzing F, Hauswald H, Bangert M. Design and selection of machine learning methods using radiomics and dosiomics for normal tissue complication probability modeling of xerostomia. Front Oncol. 2018;5:8–35. https://doi.org/10.3389/fonc.2018.00035.
56. Simon N, Friedman J, Hastie T, Tibshirani R. Regularization paths for Cox's proportional hazards model via coordinate descent. J Stat Soft. 2011;39(5):1–13. https://doi.org/10.18637/jss.v039.i05.
57. Litjens G, Kooi T, Bejnordi BE, Setio AAA, Ciompi F, Ghafoorian M, van der Laak JAWM, van Ginneken B, Sánchez CI. A survey on deep learning in medical image analysis. Med Image Anal. 2017;42:60–88.
58. Chartrand G, Cheng PM, Vorontsov E, Drozdzal M, Turcotte S, Pal CJ, Kadoury S, Tang A. Deep learning: a primer for radiologists. Radiographics. 2017;37(7):2113–31.
59. Suzuki K. Overview of deep learning in medical imaging. Radiol Phys Technol. 2017;10(3):257–73.
60. Meyer P, Noblet V, Mazzara C, Lallement A. Survey on deep learning for radiotherapy. Comput Biol Med. 2018;98:126–46.
61. Bishop CM. Pattern recognition and machine learning. New York: Springer; 2006.
62. Marcus G. Deep learning: a critical appraisal. 2018. arXiv:1801.00631v1.
63. Qin Y, Yu X, Hou J, Hu Y, Li F, Wen L, Lu Q, Fu Y, Liu S. Predicting chemoradiotherapy response of nasopharyngeal carcinoma using texture features based on intravoxel incoherent motion diffusion-weighted imaging. Medicine (Baltimore). 2018;97(30):e11676. https://doi.org/10.1097/MD.0000000000011676.
64. Wang G, He L, Yuan C, Huang Y, Liu Z, Liang C. Pretreatment MR imaging radiomics signatures for response prediction to induction chemotherapy in patients with nasopharyngeal carcinoma. Eur J Radiol. 2018;98:100–6.
65. Cui Y, Yang X, Shi Z, Yang Z, Du X, Zhao Z, Cheng X. Radiomics analysis of multiparametric MRI for prediction of pathological complete response to neoadjuvant chemoradiotherapy in locally advanced rectal cancer. Eur Radiol. 2018. https://doi.org/10.1007/s00330-018-5683-9.
66. Crispin-Ortuzar M, Apte A, Grkovski M, Oh JH, Lee NY, Schöder H, Humm JL, Deasy JO. Predicting hypoxia status using a combination of contrast-enhanced computed tomography and [18F]-Fluorodeoxyglucose positron emission tomography radiomics features. Radiother Oncol. 2018;127(1):36–42.
67. Larue RTHM, Klaassen R, Jochems A, Leijenaar RTH, Hulshof MCCM, van Berge Henegouwen MI, Schreurs WMJ, Sosef MN, van Elmpt W, van Laarhoven HWM, Lambin P. Pre-treatment CT radiomics to predict 3-year overall survival following chemoradiotherapy of esophageal cancer. Acta Oncol. 2018;1:1–7. https://doi.org/10.1080/0284186X.2018.1486039 **(Epub ahead of print)**.
68. Hou Z, Li S, Ren W, Liu J, Yan J, Wan S. Radiomic analysis in T2W and SPAIR T2W MRI: predict treatment response to chemoradiotherapy in esophageal squamous cell carcinoma. J Thorac Dis. 2018;10(4):2256–67.
69. Gangeh MJ, Hashim A, Giles A, Sannachi L, Czarnota GJ. Computer aided prognosis for cell death categorization and prediction in vivo using quantitative ultrasound and machine learning techniques. Med Phys. 2016;43(12):6439.
70. Giannini V, Mazzetti S, Marmo A, Montemurro F, Regge D, Martincich L. A computer-aided diagnosis (CAD) scheme for

pretreatment prediction of pathological response to neoadjuvant therapy using dynamic contrast-enhanced MRI texture features. Br J Radiol. 2017;90(1077):20170269. https://doi.org/10.1259/bjr.20170269.

71. Kai C, Uchiyama Y, Shiraishi J, Fujita H, Doi K. Computer-aided diagnosis with radiogenomics: analysis of the relationship between genotype and morphological changes of the brain magnetic resonance images. Radiol Phys Technol. 2018. https://doi.org/10.1007/s12194-018-0462-5.
72. Pinker K, Chin J, Melsaether AN, Morris EA, Moy L. Precision medicine and radiogenomics in breast cancer: new approaches toward diagnosis and treatment. Radiology. 2018;287(3):732–47.
73. El Naqa I. Biomedical informatics and panomics for evidence-based radiation therapy. Wiley Interdiscip Rev Data Min Knowl Discov. 2014;4:327–40.
74. Peeken JC, Bernhofer M, Wiestler B, Goldberg T, Cremers D, Rost B, Wilkens JJ, Combs SE, Nüsslin F. Radiomics in radiooncology—challenging the medical physicist. Phys Med Eur J Med Phys. 2018;48:27–36.